

***Electronic Supplementary Information (ESI)***

***for***

**Surface-engineered quantum dots/electrospun nanofibers as a  
networked fluorescent aptasensing platform toward biomarker**

**Tong Yang,<sup>a</sup> Peng Hou,<sup>a</sup> Lin Ling Zheng,<sup>a</sup> Lei Zhan,<sup>a</sup> Peng Fei Gao,<sup>a</sup> Yuan  
Fang Li,<sup>\*b</sup> and Cheng Zhi Huang<sup>\*a, b</sup>**

*<sup>a</sup> Key Laboratory of Luminescent and Real-Time Analytical Chemistry (Southwest University), Ministry of Education, College of Pharmaceutical Sciences, Southwest University, Chongqing 400715, P. R. China.*

*<sup>b</sup> Chongqing Key Laboratory of Biomedical Analysis (Southwest University), Chongqing Science & Technology Commission, School of Chemistry and Chemical Engineering, Southwest University, Chongqing 400715, P. R. China*

\* Corresponding author E-mail: [chengzhi@swu.edu.cn](mailto:chengzhi@swu.edu.cn), Tel: (+86) 23 68254659, Fax: (+86) 23 68367257.

**Table S1. Aptamer and DNA oligonucleotide sequences mainly used in this study**

Name	Sequences (5' to 3')
biotin-aptamer	ATT AAA GCT CGC CAT CAA ATA GCA AAA AAA AAA- Biotin
DNA 1	SH(CH <sub>2</sub> ) <sub>6</sub> -TTT TGC TAT TTG ATG GCG AGC TTT AAT
DNA 2	TTT TGC TAT TTG ATG GCG AGC TTT AAT-(CH <sub>2</sub> ) <sub>6</sub> SH
DNA 3	SH(CH <sub>2</sub> ) <sub>6</sub> -TTT TGC TAT TTG ATG GCG AGC TTT
DNA 4	SH(CH <sub>2</sub> ) <sub>6</sub> -TTT TGC TAT TTG ATG GCG AGC
DNA 5	SH(CH <sub>2</sub> ) <sub>6</sub> -TTT TGC TAT TTG ATG GCG

### Preparation of AuNPs and DNA-Attached AuNPs

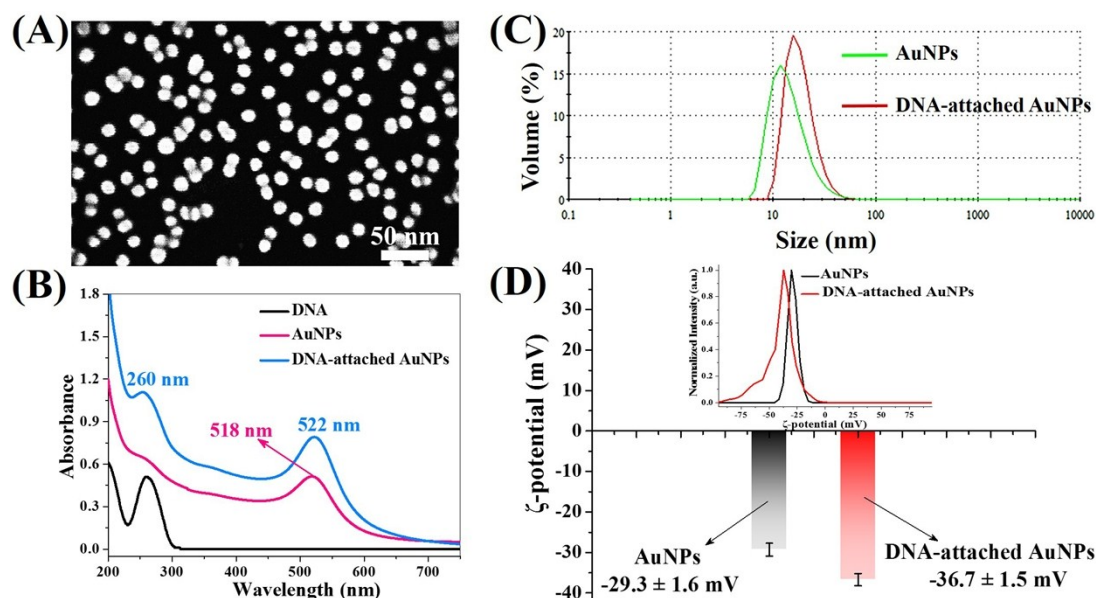


**Fig. S1** Characterizations of 13 nm AuNPs and DNA-attached AuNPs. (A) SEM image of 13 nm AuNPs, (B) localized surface plasmon resonance (LSPR) absorption spectrum, (C) hydrodynamic sizes and (D)  $\zeta$ -potentials of AuNPs and DNA-conjugated AuNPs. Inset is the original  $\zeta$ -potentials curves for AuNPs and

DNA-conjugated AuNPs.

**Note:** The morphology of the as-synthesized AuNPs were characterized by SEM (Fig. S1A). To confirm the quality of AuNPs after attaching DNA, the bare AuNPs and DNA-attached AuNPs were characterized by UV-Vis spectroscopy (Fig. S1B), which can be demonstrated that the DNA (peak at 260 nm) were conjugated on AuNPs.<sup>1</sup> Meanwhile, the spectra of DNA-attached AuNPs were almost identical for the bare AuNPs, suggesting that DNA-attached AuNPs can be also uniformly dispersed in solution based on the previous reports.<sup>2</sup> The hydrodynamic size of bare AuNPs and DNA-attached AuNPs were about 14.6 and 18.6 nm (Fig. S1C), respectively. The  $\zeta$ -potential of AuNPs after conjugating with DNA tend to more negative charges (Fig. S1D).

### Preparation of Relevant Electrospun Nanofibers

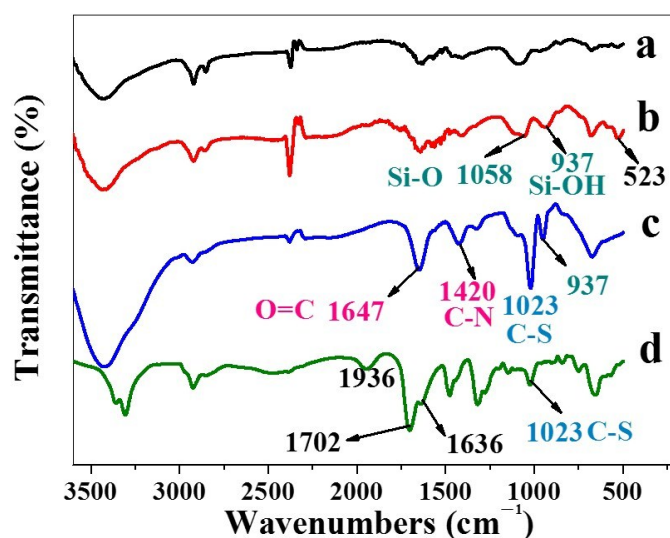


**Fig. S2** FTIR spectrum of (a) PEI/PVA NFs, (b) APTES-modified NFs, (c) biotin-grafted NFs and (d) biotin-NHS powders.

**Note:** The chemical functional groups and structural information of nanofibrous surfaces at every modification process were characterized by FTIR (Fig. S2D). Typical peaks (Fig. S2D, curves: c and d) located at 1647, 1420 and 1023  $\text{cm}^{-1}$  were attached to the stretching vibration of C=O, C-N (O=C-NH) and C-S, which can confirm that the biotin were successfully engineered on the PEI/PVA NFs.

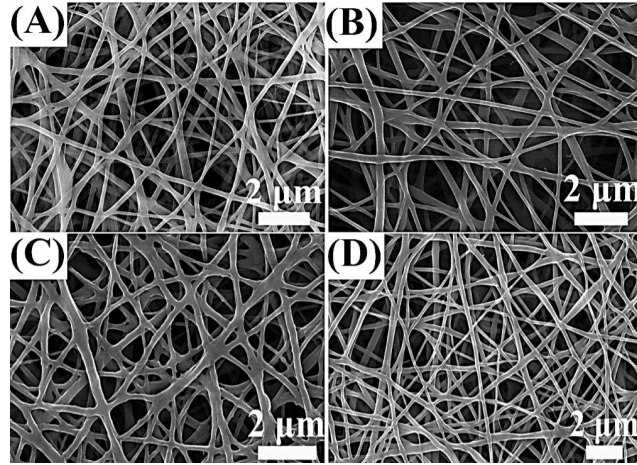


**Fig. S3** Morphology characterizations of the as-prepared electrospun nanofibers in every modified steps using chemical conjugation method. SEM images: (A) PEI/PVA NFs, (B) APTES-modified NFs, (C) biotin-grafted NFs, and (D) QDs-lighted NFs.

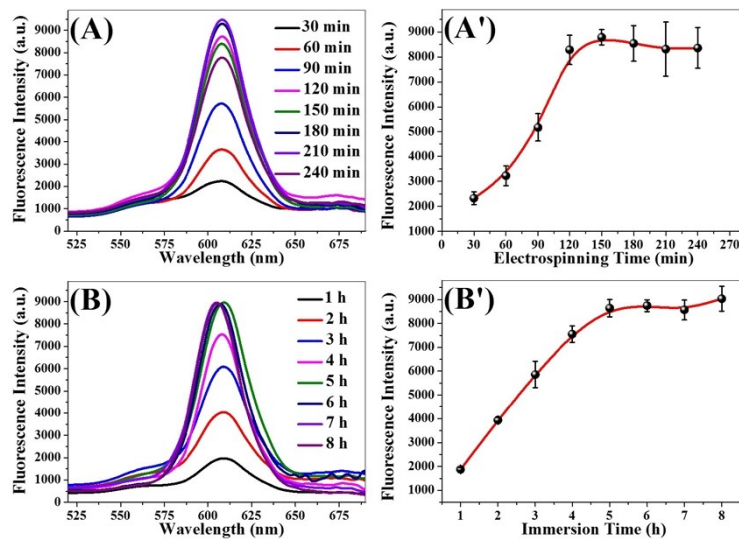


**Fig. S4** Fluorescence spectra of the as-prepared QDs-NFs. (A, A') Preparation of QDs-NFs with different electrospun times. (B, B') The biotin-modified NFs immersed in QDs@SA solution with different time.

**Note:** Considering that the thickness of the electrospun NFs and the immersion time of the biotin-modified NFs in QDs@SA solution can have an effect on the assemble contents of QDs on the surface of NFs and further influence their fluorescence intensity, the two vital factors were optimized. The fluorescence intensities of QDs-NFs became stronger with electrospinning time being prolonged, which can control the thickness of the electrospun nanofibrous membranes (Fig. S2A and A'). At the same time, the immersion time was longer

than a certain time, the fluorescence intensity of QDs-NFs were almost constant (Fig. S2B and B', ESI†). Finally, an optimized electrospinning time and immersion time were chosen as 150 min and 5 h.

### Calculation of Fluorescence lifetime decay of QDs on the relevant electrospun nanofibers

The average fluorescence lifetime of relevant QDs-NFs was calculated according to the following equation:

$$\bar{\tau} = \frac{A_1\tau_1 + A_2\tau_2 + A_3\tau_3}{A_1 + A_2 + A_3}$$

The final results are list in Table S2.

**Table S2. Fluorescence lifetime decay of QDs on the relevant electrospun nanofibers**

Sample	$\tau_1/\text{ns}$	$A_1/\%$	$\tau_2/\text{ns}$	$A_2/\%$	$\tau_3/\text{ns}$	$A_3/\%$	$\bar{\tau}$
QDs-NFs	9.24	23.2	38.0	53.2	0.43	23.6	22.5
DNA 1-AuNPs-QDs-NFs	2.62	1.02	21.4	2.08	0.063	96.9	0.53
DNA 2-AuNPs-QDs-NFs	2.80	1.50	24.4	3.40	0.063	95.1	0.93

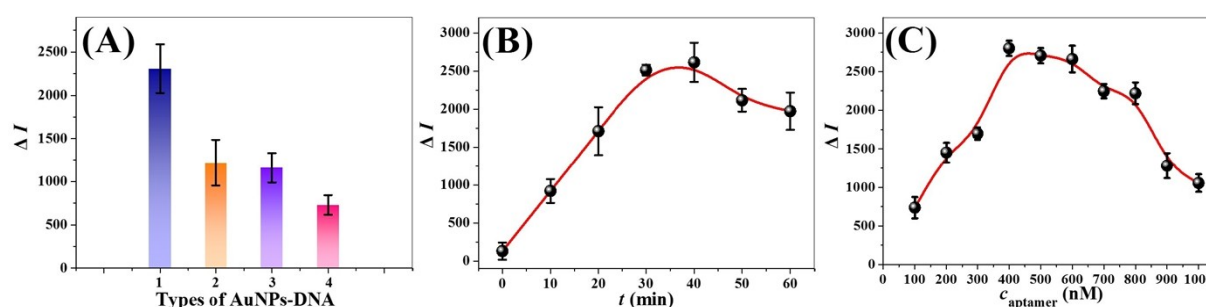


**Fig. S5** Optimization of experimental conditions. (A) Types of AuNPs-DNA with different basic groups (1, 2, 3 and 4 stand for the DNA 1, DNA 3, DNA 4 and DNA 5, respectively); (B) the immersion time of the aptamer-QDs-NFs with PSA in AuNPs-DNA solution; (C) the aptamer concentration. ( $\Delta I = I - I_{\text{control}}$ ,  $c_{\text{PSA}} = 10 \text{ ng/mL}$ ).

**Note:** To acquire an optimal analytical performance of the electrospun nanofibrous membranes-based biosensor, the different DNA-modified AuNPs, the immersion time for the aptamer-QDs-NFs in DNA-AuNPs solution, and the concentration of biotin-aptamer were optimized.

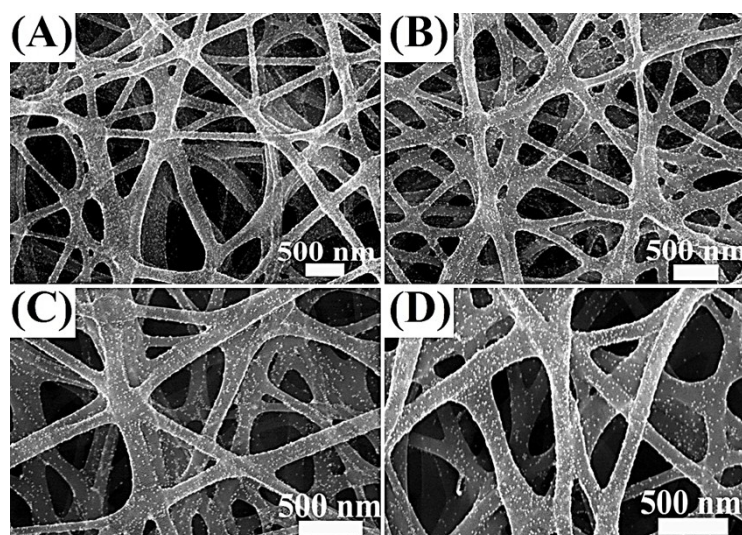


**Fig. S6** SEM images of electrospun nanofibers after using as sensing membranes for detecting PSA. (A) Control, (B) 0.01 ng/mL PSA, (C) 1 ng/mL PSA and (D) 100 ng/mL PSA.

**Note:** The concentration of PSA gradually increase together with the decreasing density of AuNPs on electrospun NFs from SEM images (Fig. S6), indicating that the rest of aptamer on QDs-NFs after capturing PSA can hybridize DNA-AuNPs.

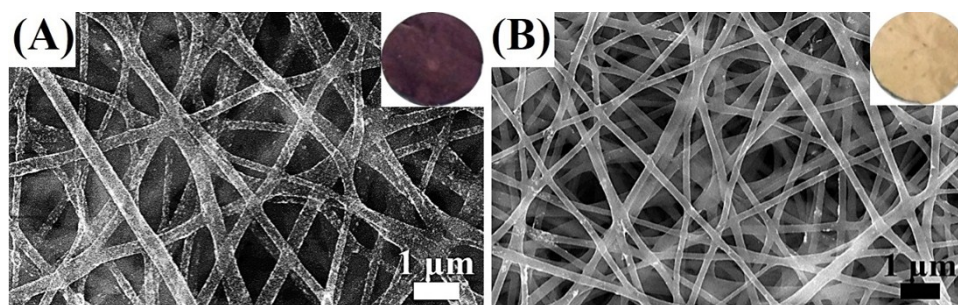


**Fig. S7** Investigation of nonspecific adsorption on sensing membranes. SEM images of aptamer-QDs-electrospun nanofibers after immersing in (A) DNA-AuNPs and (B) bare AuNPs solution.

**Note:** In order to get rid of the non-specific adsorption in sensing procedure, the aptamer-QDs-NFs were immersed into bare AuNPs solution, there are no AuNPs on the surface of aptamer-QDs-NFs (SEM images from Fig. S7).

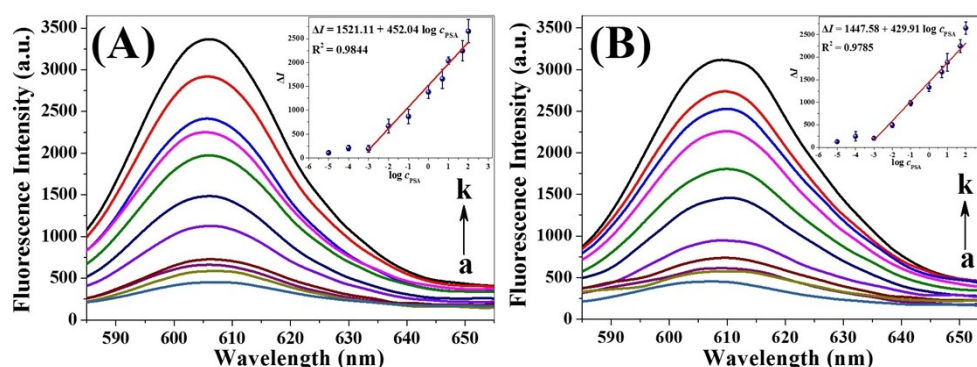


**Fig. S8** NSET-based electrospun sensing membranes with different batches for PSA detection. Fluorescence spectra of (A) batch 2 and (B) batch 3. Fluorescence spectra of the sensing electrospun membranes with different PSA solution (a) 0 (control), (b)  $1 \times 10^{-5}$ , (c)  $1 \times 10^{-4}$ , (d)  $1 \times 10^{-3}$ , (e)  $1 \times 10^{-2}$ , (f)  $1 \times 10^{-1}$ , (g) 1, (h) 5, (i) 10, (j) 50, (k) 100 ng/mL. The insets are the calibration curves for PSA analysis using two batches sensing electrospun membranes.

**Note:** The different bathes of aptamer-QDs-NFs can also displays the relatively stable fluorescent signals for the PSA detection, which can indicate the good reproducibility of the QDs-lighted electrospun sensing membranes based on NSET (Fig. S8).

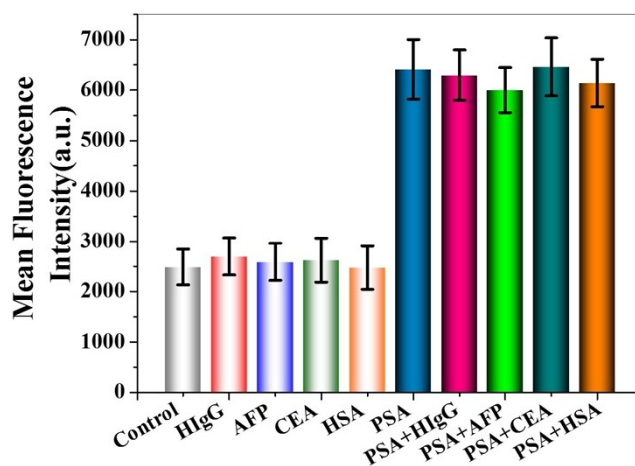


**Fig. S9** The investigation of specificity and selectivity of the aptamer-QDs-nanofibrous membranes for target PSA (0.1 ng/mL), HIgG (10 ng/mL), AFP (10 ng/mL), CEA (10 ng/mL), HSA (1000 ng/mL) and control. Statistic histograms of fluorescence intensity of the sensing nanofibrous mats from fluorescence images (Fig. 5) using IPP software.

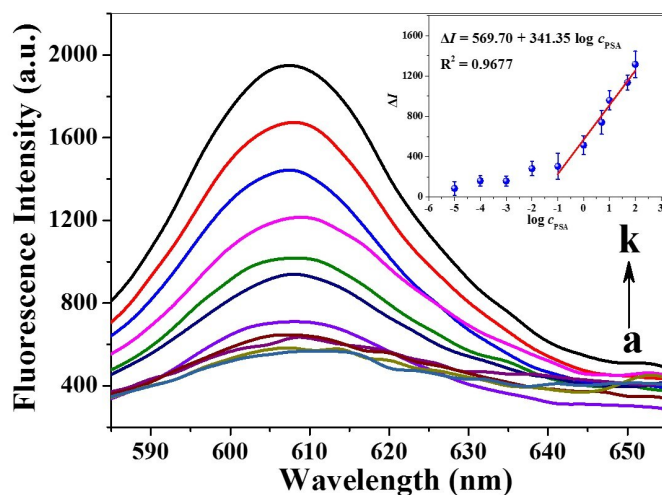


**Fig. S10** NSET-based 2D planar sensing membranes for PSA detection. Fluorescence spectra of the 2D planar sensing membranes with different PSA solution (a) 0 (control), (b)  $1 \times 10^{-5}$ , (c)  $1 \times 10^{-4}$ , (d)  $1 \times 10^{-3}$ , (e)  $1 \times 10^{-2}$ , (f)  $1 \times 10^{-1}$ , (g) 1, (h) 5, (i) 10, (j) 50, (k) 100 ng/mL. The insets are the calibration curves for PSA analysis using planar membranes.

**Note:** Comparing with the 3D electrospun aptasensing membranes, the planar sensing membranes displayed lower sensitivity for PSA detection (Fig. S10).

**Table S3. Comparison of analytical performance of the present fluorescent biosensing platform based on electrospun nanofibrous mats with other platform for PSA assay**

Detection Method	Linear Range (ng/mL)	Detection Limit	References
Chemiluminescence imaging <sup>3</sup>	0.02–125	7.0 pg/mL	[3]
Microfluidic sensor <sup>4</sup>	0.05–200	< 0.1 ng/mL	[4]
Photoelectrochemical sensor <sup>5</sup>	0.01–80	3 pg/mL	[5]
Surface enhanced Raman scattering <sup>6</sup>	—	0.5 ng/mL	[6]
Plasmonic ELISA <sup>7</sup>	0.3–5.0	9.3 pg/mL	[7]
Electrochemical immunosensor <sup>8</sup>	$10^{-5}$ –75	0.01 pg/mL	[8]
Turn-on fluorescent immunoassay <sup>9</sup>	0.001–20	0.3 pg/mL	[9]
Electrospun mats-based fluorescent	0.001–100 ng/mL	0.46 pg/mL	This work

**Table S4. Comparison experiment between electrospun sensing membranes and planar membranes for PSA assay**

Types of Membranes	Linear Range	Detection Limit
Electrospun Nanofibrous Mats	0.001–100 ng/mL	0.46 pg/mL
Planar Mats	1–100 ng/mL	0.49 ng/mL

**Note:** The detection was estimated at a signal-to-noise ratio of  $3\sigma$  (where  $\sigma$  is the standard deviation of blank sample,  $n = 11$ ).<sup>5</sup>

### References:

1. K. Zhang, T. Tan, J.-J. Fu, T. Zheng and J.-J. Zhu, *Analyst*, 2013, **138**, 6323-6330.
2. X. Zhang, M. R. Servos and J. Liu, *J. Am. Chem. Soc.*, 2012, **134**, 7266-7269.
3. A. Liu, F. Zhao, Y. Zhao, L. Shangguan and S. Liu, *Biosens. Bioelectron.*, 2016, **81**, 97-102.
4. R. Gao, Z. Cheng, A. J. deMello and J. Choo, *Lab Chip*, 2016, **16**, 1022-1029.
5. J. Shu, Z. Qiu, Q. Zhou, Y. Lin, M. Lu and D. Tang, *Anal. Chem.*, 2016, **88**, 2958-2966.
6. A. N. Ramya, M. M. Joseph, J. B. Nair, V. Karunakaran, N. Narayanan and K. K. Maiti, *ACS Appl. Mater. Interfaces*, 2016, **8**, 10220-10225.
7. L. Guo, S. Xu, X. Ma, B. Qiu, Z. Lin and G. Chen, *Sci. Rep.*, 2016, **6**, 32755.
8. M. Kukkar, S. K. Tuteja, A. L. Sharma, V. Kumar, A. K. Paul, K.-H. Kim, P. Sabherwal and A. Deep, *ACS Appl. Mater. Interfaces*, 2016, **8**, 16555-16563.
9. H. Pei, S. Zhu, M. Yang, R. Kong, Y. Zheng and F. Qu, *Biosens. Bioelectron.*, 2015, **74**, 909-914.